

# A computational setting of calcium leaching in concrete and its coupling with continuum damage mechanics

V. H. Nguyen<sup>†</sup> and B. Nedjar<sup>†</sup>

*Laboratoire d'Analyse des Matériaux et Identification, Institut Navier, 6 et 8, Avenue Blaise Pascal, Cité Descartes, Marne-la-Vallée Cedex 2, France*

J. M. Torrenti<sup>‡</sup>

*IRSN/DIR/Pg, BP 17, 92262 Fontenay-aux-Roses Cedex, France  
(Received September 17, 2003, Accepted March 23, 2004)*

**Abstract.** We present in this work a coupled phenomenological chemo-mechanical model that represents the degradation of concrete-like materials. The chemical behaviour is described by the nowadays well known simplified calcium leaching approach. And the mechanical damage behaviour is described by a continuum damage model which involves the gradient of the damage quantity. The coupled nonlinear problem at hand is addressed within the context of the finite element method. For the equation governing the calcium dissolution-diffusion part of the problem, special care is taken to treat the highly nonlinear calcium conductivity and solid calcium functions. The algorithmic design is based on a Newton-type iterative scheme where use is made of a recently proposed relaxed linearization procedure. And for the equation governing the damage part of the problem, an augmented Lagrangian formulation is used to take into account the damage irreversibility constraint. Finally, numerical simulations are compared with experimental results on cement paste.

**Keywords :** calcium leaching; continuum damage mechanics; gradient damage formulation; continuum thermodynamics; finite element method.

---

## 1. Introduction

Durability mechanics of concrete is not exclusively affected by damage induced by mechanical loads. The life-time of such a material may also depend on the environmental conditions. As a typical example, concrete is commonly employed in radioactive waste disposal, and then, concrete containment structures must ensure the load-bearing capacity over extend periods depending on the level of radioactivity (for instance 300 years for short lived low and intermediate levels radioactive waste). It is then necessary to take into account the coupling between chemical and mechanical effects when one wants to design a model to represent the behaviour of concrete for such applications.

We present in this work a chemo-mechanical modelling approach to represent the degradation

---

<sup>†</sup> Ph. D.

<sup>‡</sup> Professor

behaviour of concrete-like materials. Use is made of phenomenological descriptions for both the mechanical and chemical damage processes. On one hand, the chemical behaviour is described by the nowadays well known simplified approach of calcium leaching (see Gérard 1996, Carde, *et al.* 1996, Torrenti, *et al.* 1998b, Ulm, *et al.* 1999, Bangert, *et al.* 2001) among many other references. And on the other hand, the formalism and the evolution equations relative part are ensuing from a recently proposed formulation of the principle of virtual power where the power of the internal forces is chosen to depend, besides on the classical term involving the strain rates, also on the damage rate and the gradient of the damage rate.

This latter is introduced to account for the microscopic interactions between the material points, i.e., to take into account the influence of the damage at a material point on the damage of its neighbourhood. The first consequence of this choice is the appearance of a new boundary value problem which intends to describe the damage evolution within the solid, and which has to be solved together with the classical balance equation in solid mechanics. For a complete treatment of these latter ideas, we refer to Frémond and Nedjar (1993) and (1996), see also Nedjar (2001).

From the theoretical point of view, it is shown how the thermodynamics of irreversible processes is crucial in the characterization of the different dissipative phenomena and in setting the convenient forms of the constitutive relations.

In view of a numerical approximation, the variational formulation of the coupled problem at hand is considered in detail. Special care is taken when numerically integrating the strongly nonlinear calcium dissolution-diffusion equation (chemical part of the problem). For this, we have developed a Newton iterative algorithm involving a relaxed linearization procedure. This scheme is constructed following the same ideas as those recently proposed to solve nonlinear heat problems involving phase-change, see Nedjar (2002b) for more details. And for the damage boundary value problem (mechanical part of the problem), use is made of the algorithm developed in Nedjar (2002a), which is based on an augmented Lagrangian formulation to treat the damage irreversibility constraint. The advantage of this latter is to permit the possibility of using a monolithic (or simultaneous) scheme to solve the whole coupled problem.

An outline of the remainder of the paper is as follows. In section 2, we give the basic equations describing the coupled chemo-mechanical problem. The constitutive equations are given within the continuum thermodynamics framework and the different coupling effects are discussed in section 3. In section 4, we give a model example for the damage part of the modelling. As far as numerical formulation is concerned, a numerical design to implement the equations at hand is addressed within the context of the finite element method in section 5. The proposed framework is then evaluated numerically in section 6. Representative numerical simulations going from the calcium leaching to the mechanical loadings are compared with experimental results. And finally, conclusions and perspectives are drawn in section 7.

## **2. The coupled problem. Outlines of the balance equations**

During the last few years, different formulations have been developed to describe the coupling between chemical and mechanical effects in concrete-like materials. In this work, use is made of a phenomenological approach. We first outline the basic equation describing the calcium leaching process. Then, and for the mechanical part of the problem, we give the governing equations resulting from a recent new formulation of the principle of virtual power that accounts for the damage and gradient of damage quantities.

## 2.1. Calcium leaching part of the problem

For cement-based materials, the kinetics of calcium leaching is determined from the mass conservation of calcium which describes the evolution of the amount of calcium in the liquid phase of the material. One has the following macroscopic balance of the calcium ion mass:

$$\operatorname{div} \mathbf{q} + \dot{\phi} c + \dot{s} = 0 \quad (1)$$

where the dot  $\dot{}$  denotes the time derivative and  $\operatorname{div}[\cdot]$  is the divergence operator. And where,  $c$  denotes the calcium concentration in the liquid phase,  $s$  denotes the calcium concentration in the solid phase,  $\phi$  is the porosity in the material, and  $\mathbf{q}$  denotes the calcium mass flux vector. The rate  $\dot{s}$  denotes the calcium mass production due to the dissolution of the solid phase. According to Gérard (1996), this simplified approach focuses on the evolution of one variable only, namely: the calcium concentration  $c$ . That is, all the quantities,  $s$ ,  $\phi$  and  $\mathbf{q}$  may depend on the (state) variable  $c$ .

Typically, the function  $s(c)$  represents the equilibrium between the calcium in the solid phase  $s$  and the calcium in the liquid phase  $c$ . As an example, for the case of an accelerated calcium leaching process using ammonium nitrate, a plot of this function proposed by Tognazzi (1998) is given in Fig. 1. Two dissolution regimes are clearly distinguished: the dissolution of the portlandite and the progressive decalcification of the C-S-H.

Experimental observations also show that the porosity  $\phi$  increases with decreasing calcium concentration. Fig. 2 shows a plot of this dependence for the case of calcium leaching process also under ammonium nitrate solution. See Tognazzi (1998), Torrenti, *et al.* (1998) for example.

## 2.2. Mechanical damage part of the problem

The phenomenological response due the mechanical actions is characterized by progressive loss of stiffness with increasing loading leading to eventual failure. This degradation inevitably leads to the

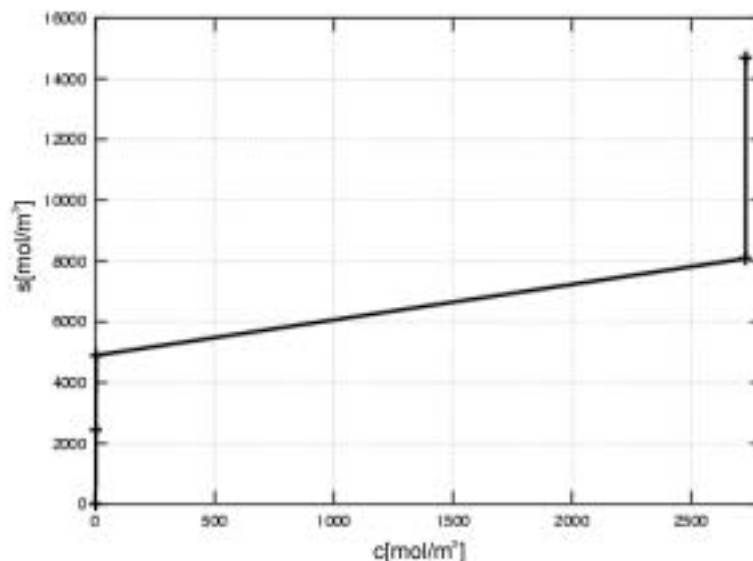


Fig. 1 Chemical equilibrium  $s(c)$  for accelerated ammonium nitrate calcium leaching

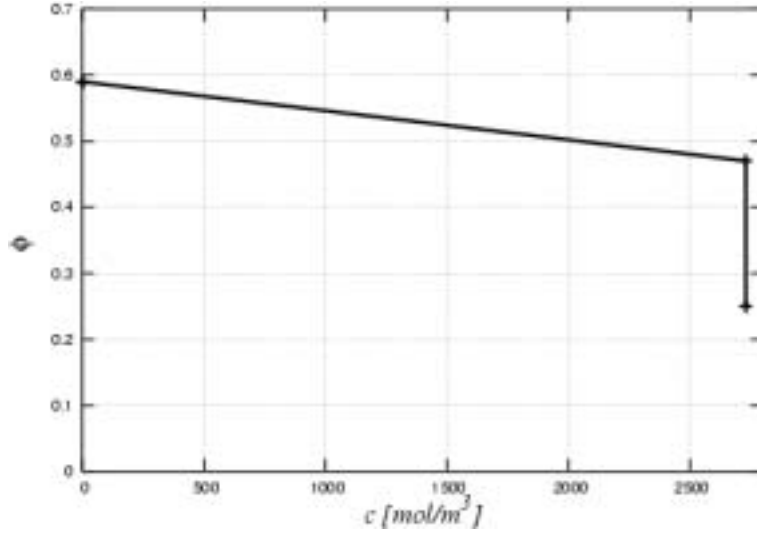


Fig. 2 Porosity  $\phi$  versus the calcium concentration  $c$

so called strain softening. And from the numerical point of view, classical local models exhibit unacceptable mesh dependence in the presence of strain softening. Several attempts have been investigated to circumvent these nowadays well known difficulties. Among the most effective enhancements, higher order formulations have been proposed by many authors these last few years. See for example Mühlhauss and Aifantis (1991), Fleck and Hutchinson (1993), Polizzoto and Borino (1998), Menzel and Steinmann (2000) among many other references.

In this work however, use is made of the gradient damage formulation developed in Frémond and Nedjar (1993), Frémond and Nedjar (1996), see also Nedjar (2001). Here we recall the main steps of this formulation. For more details, we refer to the above referenced papers.

Let the scalar  $\beta(\mathbf{x}, t)$  be the damage quantity with value 1 when the material is undamaged and value 0 when it is completely damaged. The basic idea of the theory we use is to modify the power of the internal forces  $P_{int}$  as follows. We choose this latter to depend, besides on the classical term involving the strain rates, also on the damage rate and the gradient of damage rate. For a domain  $\Omega$  with boundary  $\partial\Omega$ , we write:

$$P_{int} = - \int_{\Omega} \boldsymbol{\sigma} : \dot{\boldsymbol{\epsilon}}(\mathbf{u}) d\Omega - \int_{\Omega} (B\dot{\beta} + \mathbf{H} \cdot \text{grad} \dot{\beta}) d\Omega \quad (2)$$

where  $\boldsymbol{\sigma}$  is the stress tensor and  $\dot{\boldsymbol{\epsilon}}(\mathbf{u})$  is the strain rates tensor ( $\mathbf{u}$  being the displacement vector), and where the two non-classical quantities are:  $B$  the internal work of damage (dual to  $\beta$ ) and  $\mathbf{H}$ , the flux vector of internal work of damage (dual to  $\text{grad} \beta$ ). Taking the classical expression for the power of the external forces, the principle of virtual power in quasi-statics gives two sets of balance equations:

$$\text{div} \boldsymbol{\sigma} + \mathbf{f} = 0 \quad \text{in } \Omega \quad \boldsymbol{\sigma} \cdot \mathbf{n} = \mathbf{F} \quad \text{on } \partial\Omega \quad (3a)$$

$$\text{div} \mathbf{H} - B = 0 \quad \text{in } \Omega \quad \mathbf{H} \cdot \mathbf{n} = 0 \quad \text{on } \partial\Omega \quad (3b)$$

where  $\mathbf{n}$  is the outer unit normal to  $\partial\Omega$ ,  $\mathbf{F}$  is the prescribed superficial traction force vector and  $\mathbf{f}$  is the volumetric body force vector.

Eq. (3b) is non-classical. It is intended to describe the mechanical damage evolution within the solid. Of course, Eqs. (1) and (3) of the coupled chemo-mechanical problem need to be supplemented with constitutive relations characterizing the reversible and the dissipative responses of the solid in general. This is developed in the following.

### 3. Thermodynamic basis and constitutive relations

Due to the choice made for the power of the internal forces in Eq. (2), and confining our attention to isothermal processes, the reduced Clausius-Duhem dissipative inequality now takes the form:

$$D = \boldsymbol{\sigma}:\dot{\boldsymbol{\epsilon}} + B\dot{\beta} + \mathbf{H}\cdot\mathbf{grad}\dot{\beta} + \mu\dot{c} - \mathbf{q}\cdot\mathbf{grad}\mu - \dot{\psi} \geq 0 \quad (4)$$

which must be satisfied for any admissible process. In Eq. (4),  $\psi$  denotes the free energy function which characterizes the state of the material and which has to be specified.  $\mu$  is the chemical potential of calcium associated to the calcium concentration  $c$ .

As the state of the material is characterized by its free energy  $\psi$ , it is then natural to assume that this latter depends also on the damage quantity  $\beta$  and its gradient. Assuming for the sake of clarity that there is no dissipation due to plasticity, the free energy function is chosen to be of the general form:  $\psi \equiv \psi(\boldsymbol{\epsilon}, \beta, \mathbf{grad}\beta, c)$ . Substituting this latter into Eq. (4) and using the Coleman's method, see for example Coleman and Gurtin (1967), one obtains that the following three inequalities must be satisfied:

$$D_1 = \left( \boldsymbol{\sigma} - \frac{\partial\psi}{\partial\boldsymbol{\epsilon}} \right) : \dot{\boldsymbol{\epsilon}} + \left( \mu - \frac{\partial\psi}{\partial c} \right) \dot{c} \geq 0 \quad (5)$$

$$D_2 = \left( \mathbf{H} - \frac{\partial\psi}{\partial(\mathbf{grad}\beta)} \right) \cdot \mathbf{grad}\dot{\beta} + \left( B - \frac{\partial\psi}{\partial\beta} \right) \dot{\beta} \geq 0 \quad (6)$$

$$D_3 = -\mathbf{q}\cdot\mathbf{grad}\mu \geq 0 \quad (7)$$

In Eq. (6),  $D_2$  represents the dissipation due to damage. Inequalities Eqs. (5) and (6) give:

$$\boldsymbol{\sigma} = \frac{\partial\psi}{\partial\boldsymbol{\epsilon}} \quad (8a)$$

$$\mu = \frac{\partial\psi}{\partial c} \quad (8b)$$

$$\mathbf{H} = \frac{\partial\psi}{\partial(\mathbf{grad}\beta)} \quad (8c)$$

together with the reduced inequality

$$D_2 = \left( B - \frac{\partial\psi}{\partial\beta} \right) \dot{\beta} \geq 0 \quad (9)$$

Noting that this latter must be strict when damage occurs, i.e., if  $\dot{\beta} \neq 0$  then  $D_2 \neq 0$  strictly, the choice  $B = \frac{\partial\psi}{\partial\beta}$  is then unacceptable. We postulate then the existence of a damage potential of

dissipation  $\chi(\beta, \dots)$ , i.e., a positive, convex and sub-differentiable function with  $\chi = 0 \Leftrightarrow \beta = 0$ , such that

$$B - \frac{\partial \psi}{\partial \beta} = \frac{\partial \chi}{\partial \beta}, \Rightarrow B = \frac{\partial \psi}{\partial \beta} + \frac{\partial \chi}{\partial \beta} \quad (10)$$

The convexity of  $\chi$  is then sufficient to satisfy the inequality Eq. (9) (and hence Eq. (6)) for any admissible process. Note that in the definition of  $\chi$ ,  $\beta$  is the lonely argument and other variables have the possibility to act as (fixed) parameters.

In Eq. (7),  $D_3$  represents the dissipation due to the diffusion of calcium. Following similar arguments as in Gérard (1996), use of the Fick's law together with the relation Eq. (8b), leads to the following constitutive relation for the calcium mass flux vector:

$$\mathbf{q} = -\tilde{D}(c)\mathbf{grad}c \quad (11)$$

where  $\tilde{D}(c)$  is the apparent calcium ion conductivity. With this latter, the calcium diffusion problem to be solved is obtained by substituting Eq. (11) into (1) to give:

$$\overline{(\phi(c)c)} + \dot{s}(c) = \text{div}[\tilde{D}(c)\mathbf{grad}c] \quad (12)$$

This equation is highly nonlinear. On one hand, because of the relations  $s(c)$  and  $\phi(c)$  plotted in Figs. 1 and 2, respectively. And on the other hand, because the apparent calcium conductivity  $\tilde{D}(c)$  also depends nonlinearly on  $c$ . As an example, a plot of this dependence is shown in Fig. 3 for the case of calcium leaching using ammonium nitrate (Tognazzi 1998).

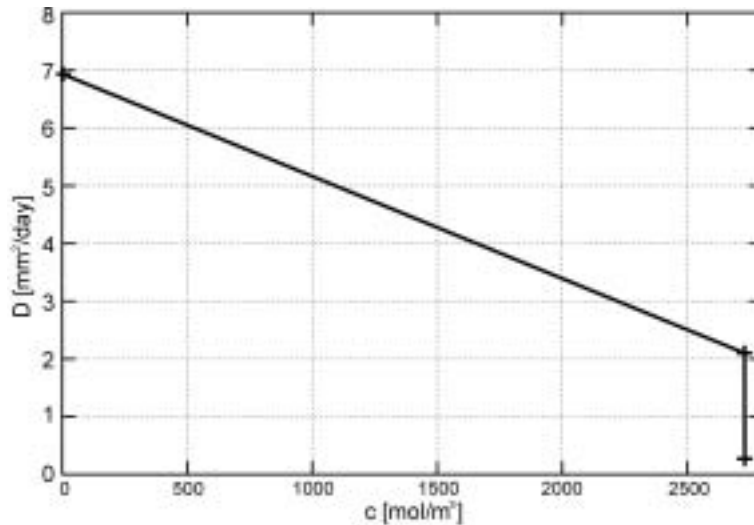


Fig. 3 Apparent conductivity  $\tilde{D}$  versus the calcium concentration  $c$

### 3.1. Chemo-mechanical couplings

The interactions between calcium leaching and mechanical damage have been investigated by many authors, (see Gérard 1996, Carde 1996, Torrenti, *et al.* 1999, Ulm, *et al.* 1999, Bangert, *et al.* 2001, Le Bellégo, *et al.* 2001) among others. On one hand, calcium leaching leads to a decrease of mechanical properties. And on the other hand, mechanical damage increases the apparent conductivity of the calcium in the liquid phase (Torrenti, *et al.* 1998a).

However, and for the sake of simplicity, this latter effect will not be considered for the moment in the present work. Here we consider only the case where calcium leaching affects the mechanical properties of the material, i.e., coupling in the direction chemical to mechanical. As an illustration, Fig. 4 shows how the calcium concentration affects the Young's modulus  $E(c)$  of a cement-based material (Torrenti, *et al.* 1998a).

Of course, the coupling in the other direction, i.e., in the direction mechanical to chemical, is important to consider too. This will be investigated in future works when fully coupled numerical treatment will be developed.

## 4. An elastic-damage model

To make matters as concrete as possible, we give in this section an elastic-damage model. For the mechanical part of the free energy function  $\psi$ , we choose the following form already studied in Nedjar (2001, 2002a) :

$$\psi_{mech} = \frac{1}{2} \beta \boldsymbol{\varepsilon} : \mathbf{C}(c) : \boldsymbol{\varepsilon} + \frac{1}{2} k (\mathbf{grad} \beta)^2 \quad (13)$$

where the first term constitutes the simplest model where damage is coupled to elasticity,  $\mathbf{C}(c)$  is the classical rank four Hooke's elasticity tensor ( $\lambda(c)$  and  $\mu(c)$  being the Lamé coefficients) where the Young's modulus  $E(c)$  is given, for instance, by Fig. 4. And in the second term,  $k$  is the factor

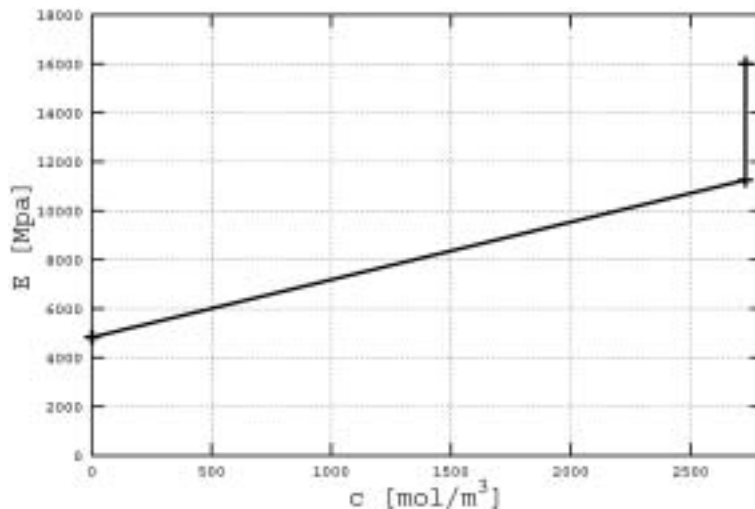


Fig. 4 Young's modulus  $E$  as a function of the calcium concentration  $c$

of influence of damage gradient.

For the damage dissipation function  $\chi$  in Eq. (10), we choose the following rate-independent damage form (also proposed in Nedjar 2001, 2002a) :

$$\chi(\dot{\beta}) = -\dot{\beta} \left[ W(c) + \frac{1}{2} \boldsymbol{\epsilon} : \mathbf{C}(c) : \boldsymbol{\epsilon} - \beta^n S(\boldsymbol{\epsilon}) \right] + I_-(\dot{\beta}) \quad (14)$$

where  $W(c)$  is the initial damage threshold which here depends on the calcium concentration  $c$ ,  $n > 0$  is a parameter that controls the hardening/softening material behaviour. When  $n > 2$ , the material exhibits hardening while when  $n < 2$  it exhibits softening.  $S(\boldsymbol{\epsilon})$  is a source of damage which depends on the mechanisms that govern the damage growth within the material, and  $I_-(\dot{\beta})$  is the indicator function of the subset  $[-\infty, 0]$  which forces  $\dot{\beta}$  to be negative or zero valued ( $I_-(x) = 0$  if  $x \leq 0$  and  $I_-(x) = +\infty$  if  $x > 0$ ). This latter is introduced to take into account the fact that damage is an irreversible process.

The choice of the source of damage function  $S(\boldsymbol{\epsilon})$  is not unique. It can depend on the total deformation or part of it following the material under consideration. Here  $S(\boldsymbol{\epsilon})$  depends on the positive strains as proposed in Nedjar (2001) and as it will be seen later in section 6.2.

Substitution of Eqs. (13) and (14) into Eqs. (8a), (8c) and (10) gives:

$$\boldsymbol{\sigma} = \beta \mathbf{C}(c) : \boldsymbol{\epsilon} \quad (15a)$$

$$\mathbf{H} = k \mathbf{grad} \beta \quad (15b)$$

$$B \in \beta^n \psi(\boldsymbol{\epsilon}, c) - W(c) + \partial I_-(\dot{\beta}) \quad (15c)$$

In Eq. (15c),  $\partial I_-(\dot{\beta})$  is the generalized derivative of  $I_-(\dot{\beta})$ . It is a mathematical reaction which forces  $\dot{\beta}$  to be negative or equal to zero, i.e.,  $\partial I_-(x) = \{0\}$  if  $x < 0$  and  $\partial I_-(0) = [0, +\infty]$ .

Then, substitution of the last results into Eq. (3) gives the equations of the mechanical part of the problem:

$$\begin{aligned} \operatorname{div}(\beta \mathbf{C}(c) : \boldsymbol{\epsilon}) + \mathbf{f} &= 0 & \text{in } \Omega \\ \boldsymbol{\sigma} \cdot \mathbf{n} &= \mathbf{F} & \text{on } \partial\Omega \end{aligned} \quad (16)$$

$$-k\Delta\beta + \beta^n S(\boldsymbol{\epsilon}) + \partial I_-(\dot{\beta}) \ni W(c) \quad \text{in } \Omega \quad (17a)$$

$$k \mathbf{grad} \beta \cdot \mathbf{n} = 0 \quad \text{on } \partial\Omega \quad (17b)$$

where  $\Delta$  denotes the Laplacian operator.

Note that within the present work, the chemo-mechanical coupling is present only through the Young's modulus  $E(c)$  and the damage threshold  $W(c)$ . For the application that follows,  $E(c)$  is given by Fig. 4, and  $W(c) = W_0 (E(c)/E_0)$ , where  $E_0$  and  $W_0$  are the respective initial values of  $E(c)$  and  $W(c)$  when no leaching and no damage occur.

## 5. Variational formulation and numerical design

The variational formulations of the local form of the governing Eqs. (12), (16) and (17) play a central role in the numerical solution of the coupled boundary value problem. As the calcium leaching is a slow process, we choose to decouple the chemical and the mechanical parts of the problem in the actual numerical implementation. That is, the transient problem of calcium leaching is solved first to obtain the calcium concentration field. Then, this latter is injected into the coupled elastic-damage sub-problem to obtain the displacement and damage fields. Of course, a fully coupled resolution of the field equations can easily be performed from the developments that follow. We first describe the numerical resolution of the calcium leaching problem. The elastic-damage sub-problem is treated next.

### 5.1. The calcium leaching part of the problem

The weak form of the calcium dissolution-diffusion Eq. (12) is given by:

$$\int_{\Omega} \delta c \frac{\partial \tilde{S}(c)}{\partial t} d\Omega + \int_{\Omega} \mathbf{grad} \delta c \cdot \tilde{D}(c) \mathbf{grad} c d\Omega = 0 \quad (18)$$

which must hold for all admissible variations  $\delta c$ . For simplicity, Dirichlet boundary conditions are assumed on the entire boundary  $\partial\Omega$ . Here and in all what follows we adopt the notation

$$\tilde{S}(c) = s(c) + \phi(c)c \quad (19)$$

which is a given function together with  $\tilde{D}(c)$ .

Many strategies have been developed to solve this problem. The numerical resolution is based on an iterative procedure of the discrete version of Eq. (18). Typically, this requires a linearization and, accordingly, one solves a sequence of successive linear problems. However, one can expect severe numerical difficulties and use of refined mesh is necessary because of the strong nonlinearities exhibited by  $\tilde{S}(c)$  and  $\tilde{D}(c)$  functions, see Figs. 1 to 3. Another way is to treat this equation as a Stefan-like problem as in Ulm, *et al.* (2002), or resolve it via the finite volumes method as in Mainguy, *et al.* (2000). In this work however, and motivated by a recent algorithm proposed in Nedjar (2002b) within the context of nonlinear heat problems involving phase change, we employ the relaxed linearization as described next.

#### 5.1.1. Relaxed linearization

The procedure will concern the highly nonlinear functions  $\tilde{S}(c)$  and  $\tilde{D}(c)$ . The key idea proceeds in three steps:

°In the first step, use is made of the reciprocal forms of the precedent two functions. That is, we introduce the new functions:

$$c = f(\tilde{S}) \quad \text{and} \quad c = g(\tilde{D}) \quad (20)$$

which can be easily deduced from  $\tilde{S}(c)$  and  $\tilde{D}(c)$ , respectively.

◦In the second step, the linearizations of the above functions  $f$  and  $g$  are given by:

$$\begin{aligned} c^{(i+1)} &= f(\tilde{S}^{(i)}) + f'(\tilde{S}^{(i)})\Delta\tilde{S}^{(i)} \\ c^{(i+1)} &= g(\tilde{D}^{(i)}) + g'(\tilde{D}^{(i)})\Delta\tilde{D}^{(i)} \end{aligned} \quad (21)$$

where  $c^{(i+1)} = c^{(i)} + \Delta c^{(i)}$ ,  $\Delta\tilde{S}^{(i)} = \tilde{S}^{(i+1)} - \tilde{S}^{(i)}$ ,  $\Delta\tilde{D}^{(i)} = \tilde{D}^{(i+1)} - \tilde{D}^{(i)}$ , and where  $f'$  and  $g'$  are the derivatives of  $f$  and  $g$  with respect to their argument. The superscripts  $(i)$  and  $(i+1)$  refer to the iteration number.

The identities (21) are equivalently written as:

$$\begin{aligned} \Delta\tilde{S}^{(i)} &= \frac{1}{f'(\tilde{S}^{(i)})} [\Delta c^{(i)} + (c^{(i)} - f(\tilde{S}^{(i)}))] \\ \Delta\tilde{D}^{(i)} &= \frac{1}{g'(\tilde{D}^{(i)})} [\Delta c^{(i)} + (c^{(i)} - g(\tilde{D}^{(i)}))] \end{aligned} \quad (22)$$

◦And in the third step, the latter incrementations (22) are relaxed by replacing the quantities  $1/(f'(\tilde{S}^{(i)}))$  and  $1/(g'(\tilde{D}^{(i)}))$  by constant quantities  $\mu$  and  $\gamma$  in all the domain and during the whole iterative process as:

$$\begin{aligned} \Delta\tilde{S}^{(i)} &= \mu[\Delta\tilde{c}^{(i)} + (c^{(i)} - f(\tilde{S}^{(i)}))] \\ \Delta\tilde{D}^{(i)} &= \gamma[\Delta\tilde{c}^{(i)} + (c^{(i)} - g(\tilde{D}^{(i)}))] \end{aligned} \quad (23)$$

The relaxation parameters and must satisfy the respective conditions:

$$\mu \leq \frac{1}{\max f'(\tilde{S}^{(i)})}, \quad \gamma \leq \frac{1}{\max g'(\tilde{D}^{(i)})} \quad (24)$$

where  $f'(\tilde{S}^{(i)})$  and  $g'(\tilde{D}^{(i)})$  are determined from the  $f'(\tilde{S}^{(i)})$  and  $g'(\tilde{D}^{(i)})$  curves. In our numerical examples, we use  $\mu = 1/\max f'(\tilde{S}^{(i)})$  and  $\lambda = 1/\max g'(\tilde{D}^{(i)})$ .

### 5.1.2. Resolution algorithm for the calcium leaching part of the problem

To solve the problem Eq. (18) using the precedent algorithmic procedure, we first perform a finite difference scheme in time. In this paper, use is made of a backward-Euler scheme as follows. Consider a typical time subinterval  $[t_n, t_{n+1}]$ , then, starting from a known converged state  $(c_n, \tilde{S}_n, \tilde{D}_n)$  at time  $t_n$ , we look for the new state  $(c_{n+1}, \tilde{S}_{n+1}, \tilde{D}_{n+1})$  at time  $t_{n+1}$  by solving:

$$\int_{\Omega} \delta c \frac{\tilde{S}_{n+1}}{\Delta t} d\Omega + \int_{\Omega} \mathbf{grad} \delta c \cdot \tilde{D}_{n+1} \mathbf{grad} c_{n+1} d\Omega = \int_{\Omega} \delta c \frac{\tilde{S}_n}{\Delta t} d\Omega \quad (25)$$

where  $\Delta t = t_{n+1} - t_n$ . A classical linearization of Eq. (25) gives:

$$\int_{\Omega} \delta c \frac{\tilde{S}_{n+1}^{(i)}}{\Delta t} d\Omega + \int_{\Omega} \mathbf{grad} \delta c \cdot \mathbf{grad} c_{n+1}^{(i)} \Delta\tilde{D}_{n+1}^{(i)} d\Omega + \int_{\Omega} \mathbf{grad} \delta c \tilde{D}_{n+1}^{(i)} \mathbf{grad} \Delta c_{n+1}^{(i)} d\Omega = R_{n+1}^{(i)} \quad (26)$$

where the residual  $R_{n+1}^{(i)}$  at iteration ( $i$ ) is given by:

$$R_{n+1}^{(i)} = \int_{\Omega} \delta c \frac{\tilde{S}_n - \tilde{S}_{n+1}^{(i)}}{\Delta t} d\Omega - \int_{\Omega} \mathbf{grad} \delta c \tilde{D}_{n+1}^{(i)} \mathbf{grad} \Delta c_{n+1}^{(i)} d\Omega \quad (27)$$

In Eqs. (26) and (27), subscripts refer to the time step and superscripts refer to the iteration within the time step.

The relaxed linearization of the problem Eq.(18) is then obtained by replacing the incrementations Eq. (23) into the first and second terms of the left hand side of Eq. (26) giving:

$$\begin{aligned} & \int_{\Omega} \delta c \mu \frac{\Delta c_{n+1}^{(i)}}{\Delta t} d\Omega + \int_{\Omega} \mathbf{grad} \delta c \cdot \mathbf{grad} c_{n+1}^{(i)} \Delta c_{n+1}^{(i)} d\Omega + \int_{\Omega} \mathbf{grad} \delta c \tilde{D}_{n+1}^{(i)} \mathbf{grad} \Delta c_{n+1}^{(i)} d\Omega \\ & = R_{n+1}^{(i)} - \int_{\Omega} \delta c \frac{\mu \Delta}{\Delta t} (c_{n+1}^{(i)} - f(\tilde{S}_{n+1}^{(i)})) d\Omega - \int_{\Omega} \mathbf{grad} \delta c \cdot \mathbf{grad} c_{n+1}^{(i)} \gamma (c_{n+1}^{(i)} - g(\tilde{D}_{n+1}^{(i)})) d\Omega \end{aligned} \quad (28)$$

At the end of each iteration, the updating procedure is accomplished as follows:

$$c_{n+1}^{(i+1)} = c_{n+1}^{(i)} + \Delta c_{n+1}^{(i)} \quad (29a)$$

$$\tilde{S}_{n+1}^{(i+1)} = \tilde{S}_{n+1}^{(i)} + \mu (c_{n+1}^{(i+1)} - f(\tilde{S}_{n+1}^{(i)})) \quad (29b)$$

$$\tilde{D}_{n+1}^{(i+1)} = \tilde{D}_{n+1}^{(i)} + \gamma (c_{n+1}^{(i+1)} - g(\tilde{D}_{n+1}^{(i)})) \quad (29c)$$

From the finite element point of view, the update (29a) is accomplished at the nodal level while the updates Eqs. (29a) and (29c) are performed at the integration points. For completeness, Table 1 summarizes the algorithmic iterative scheme to solve the calcium leaching part of the problem.

Table 1 Numerical design to solve the calcium leaching part of the problem

---

**1. Initialization from a converged solution**

at  $t = t_n$ :  $i = 0$ ,  $c_{n+1}^{(0)} = c_n$ ,  $\tilde{S}_{n+1}^{(0)} = \tilde{S}_n$ ,  $\tilde{D}_{n+1}^{(0)} = \tilde{D}_n$ .

**2. Integrate the element matrices and residuals from Eq. (28) and Eq. (27)**

**3. Assemble and solve for a new calcium concentration increment:  $\Delta c_{n+1}^{(i)}$**

**4. Update the nodal values of calcium concentration by using the update (29a)**

**5. Update locally at each integration point by using the formulae (29b) and (29c)**

**6. Set  $i \leftarrow i+1$  and go to 2**

---

## 5.2. The elastic-damage part of the problem

Following standard arguments, the two sets of balance Eqs. (16) and (17) are equivalent to the following two weak forms:

$$\int_{\Omega} \nabla^s(\delta \mathbf{u}) : \mathbf{C}(c) : \nabla^s(\mathbf{u}) d\Omega = G_{ext}(\delta \mathbf{u}) \quad (30)$$

$$\int_{\Omega} \mathbf{grad}(\delta \beta) \cdot k \mathbf{grad} \beta d\Omega + \int_{\Omega} \delta \beta \beta^n S(\varepsilon) d\Omega = \int_{\Omega} \delta \beta W(c) d\Omega \quad (31a)$$

$$\text{with } \dot{\beta}(\mathbf{x}, t) \leq 0 \quad \forall \mathbf{x} \in \Omega, \forall t \quad (31b)$$

which must hold for all admissible variations  $\delta \mathbf{u}$  and  $\delta \beta$ , of  $\mathbf{x}$  displacement and damage, respectively. In Eq. (30),  $G_{ext}(\delta \mathbf{u})$  is a short hand notation for the virtual work of the external loading, and  $\nabla^s$  denotes the symmetric gradient operator. In Eq. (31a) the imposition of the constraint reflects the presence of the mathematical reaction in Eq. (31b) reflects the presence of the mathematical reaction  $\partial I_-(\dot{\beta})$  in Eq. (17a).

The strategy we use to solve numerically this problem is the one proposed in Nedjar (2002a) within the context of geometrically nonlinear problems, and that improves the one used in Nedjar (2001), Frémond and Nedjar (1996). Here the constraint Eq. (31b) is treated with an augmented Lagrangian technique as show below.

### 5.2.1. Augmented Lagrangian formulation for the damage part

In order to circumvent the restriction imposed by the presence of the constraint Eq. (31b), we first introduce an additional variable  $r$  over  $\Omega$  and which we define as the damage history variable:

$$r(\mathbf{x}, t) = \min_{\tau \leq t} \beta(\mathbf{x}, \tau) \quad (32)$$

Next, the constraint (31b) is replaced by the following equivalent one:

$$\beta(\mathbf{x}, t) - r(\mathbf{x}, t) \leq 0, \quad \forall \mathbf{x} \in \Omega, \forall t \quad (33)$$

Then, the damage part of the problem Eq. (31a) subject to the constraint Eq. (33) is equivalently rewritten in the following (single) form corresponding to a penalty formulation:

$$\int_{\Omega} \mathbf{grad}(\delta \beta) k \mathbf{grad} \beta d\Omega + \int_{\Omega} \delta \beta \beta^n S \boldsymbol{\varepsilon} d\Omega - \int_{\Omega} \delta \beta \varepsilon (\beta - r) d\Omega = \int_{\Omega} \delta \beta W(c) d\Omega \quad (34)$$

where  $\varepsilon$  is a fixed penalty parameter, and where  $\langle . \rangle$  is the positive part function defined as  $\langle x \rangle = 1/2[x + |x|]$ . This new form is extremely attractive for finite element implementations. However, it is well-known that worsens as the penalty value  $\varepsilon$  increases.

This led us to turn to the following alternative approach involving augmented Lagrangian technique. Starting with the variational form Eq. (34), we append a penalty regularization procedure which renders the following form:

$$\int_{\Omega} \mathbf{grad}(\delta \beta) k \mathbf{grad} \beta d\Omega + \int_{\Omega} \delta \beta \beta^n S(\boldsymbol{\varepsilon}) d\Omega + \int_{\Omega} \delta \beta \langle \eta + \varepsilon(\beta - r) \rangle d\Omega = \int_{\Omega} \delta \beta W(c) d\Omega \quad (35)$$

where the additional variable  $\eta$  is a parameter, and where one can note that the term  $\langle \eta + \varepsilon(\beta - r) \rangle$  plays the role of an exact Lagrangian multiplier. The idea of this method is to search the correct  $\eta$  in an iterative process. Eq. (35) is solved with fixed current estimate  $\eta^{(k)} \geq 0$  of  $\eta$  at iteration ( $k$ ) and then, use is made of the following update formula

$$\eta^{k+1} = \langle \eta^k + \varepsilon(\beta - r) \rangle \quad (36)$$

This update procedure has been motivated by a similar strategy developed in Simo and Laursen

(1992) for the treatment of frictionless contact problems.

Notice that it is also necessary to solve the coupled problem, now given by Eqs. (30) and (35), in an iterative manner. In this work, use is made of the nested iterative scheme, as referred to in Simo and Laursen 1992). That is, the coupled problem Eqs. (30) and (35) is solved completely before the update Eq. (36) is performed. For the sake of clarity, Table 2 summarizes the conceptual steps involved during the resolution. Recall that within this step of resolution, the calcium concentration  $c$  is considered as a fixed field.

**Remark 1** In the scheme considered here,  $\varepsilon$  is fixed during the procedure. In practice  $\varepsilon$  is chosen to be as large as possible without including ill-conditioning. The satisfaction of the constraint Eq. (32) (or equivalently Eq. (31b)) can be improved even if  $\varepsilon$  is undersized through repeated application of the augmentation procedure Eq. (36) which only changes  $\eta^{(k)}$ .

**Remark 2** The advantage of the present resolution strategy is, on one hand, the possibility to use a simultaneous scheme to solve the coupled equations in the inner-loop step (step 2 of Table 2) and, on the other hand, to preserve the structure of the actual algorithmic treatments elastic-damage and elastoplastic-damage problems widely investigated in the literature.

Table 2 Nested augmented Lagrangian scheme for the elastic-damage part of the problem

---

**1. Initialization:**  
Set  $\eta^0 = \eta + \langle \varepsilon(\beta - r) \rangle$  from the last step,  $k=0$ .  
**2. Solve the coupled Eqs. (30) and (35) for  $u^{(k)}$  and  $\beta^{(k)}$**   
**3. Check for constraint satisfaction**  
IF  $(\beta^k(\mathbf{x}) - r^k(\mathbf{x}) \leq TOL, \forall x \in \Omega,)$  THEN  
Convergence. EXIT  
ELSE Augment :  $\eta^{k+1} = \langle \eta^k + \varepsilon(\beta^k - r) \rangle$  set  $k \leftarrow k + 1$   
GOTO2 END IF

---

Within the inner-loop in step 2 of Table 2, the coupled nonlinear Eqs. (30) and (35) are solved here by means of the Newton-Raphson method. Accordingly, this requires the linearization of these equations about a known state  $\{\mathbf{u}, \beta\} = \{\mathbf{u}^{(i)}, \beta^{(i)}\}$  at each inner iteration ( $i$ ). This is performed directly in the finite element discretization that follows.

### 5.3. Finite element discretization of the elastic-damage part

From the nature of the governing Eqs. (30) and (35), damage is treated as a continuous field. From the finite element viewpoint, damage is required at the nodal level. Moreover, the same shape functions are used for the displacement and the damage fields. As usual, consider a discretization of the domain  $\Omega \subset R^n$  ( $n = 2$  or  $3$  is the space dimension) into a collection of finite elements  $\Omega_e$ . The interpolations of the displacement and damage fields over a typical element take the form:

$$\mathbf{u}_e(\zeta, t) = \sum_{A=1}^{n_{nodes}} N^A(\zeta) \mathbf{d}_A^e(t), \quad \beta_e(\zeta, t) = \sum_{A=1}^{n_{nodes}} N^A(\zeta) \beta_A^e(t), \quad (37)$$

where  $\mathbf{d}_A^e \in R^n$  and  $\beta_A^e(t) \in R$  denote the nodal displacements and damage, respectively, associated with node  $N^A(\zeta)$  are the shape functions. Here the coupled elastic-damage sub-problem is solved

by using a simultaneous scheme. The element contributions to the tangent stiffness matrix associated with the element nodes are written as:

$$\mathbf{K}_e^{AB} = \begin{bmatrix} \mathbf{K}_{e_{11}}^{AB} & \mathbf{K}_{e_{12}}^{AB} \\ \mathbf{K}_{e_{21}}^{AB} & \mathbf{K}_{e_{22}}^{AB} \end{bmatrix} \in R^{(n+1) \times (n+1)} \quad (38)$$

for  $A, B=1, \dots, n_{\text{node}}^e$ . In this matrix, the first column (row) is associated with the  $n$  components of the nodal displacements while the second column (row) is associated with the nodal damage. The expressions of the sub-matrices are given by:

$$\mathbf{K}_{e_{11}}^{AB} = \int_{\Omega^e} \mathbf{B}[N^A]^T \beta \mathbf{C}(c) \mathbf{B}[N^B] d\Omega_e, \quad (39a)$$

$$\mathbf{K}_{e_{11}}^{AB} = \int_{\Omega^e} \mathbf{B}[N^A]^T \beta \mathbf{C}(c) : \varepsilon N^B d\Omega_e, \quad (39b)$$

$$\mathbf{K}_{e_{21}}^{AB} = \int_{\Omega^e} N^A \beta^n \frac{\partial S(\varepsilon)}{\partial \varepsilon} \mathbf{C}(c) \mathbf{B}[N^B] d\Omega_e, \quad (39c)$$

$$\mathbf{K}_{e_{22}}^{AB} = \int_{\Omega^e} \nabla[N^A]^T \cdot k \cdot \nabla N^B d\Omega_e + \int_{\Omega^e} N^A \{n \beta^{(n-1)} S(\varepsilon) + \varepsilon \tilde{H}\} N^B d\Omega_e \quad (39d)$$

where  $\nabla N^A$  and  $\mathbf{B}[N^A]$  are the usual discrete gradient and symmetric gradient operators, respectively. In the expression of  $\mathbf{K}_{e_{22}}^{AB}$  in Eq. (39d),  $H$  is an homographic approximation of the Heaviside function to avoid evident numerical difficulties:

$$H(x) = \frac{1}{2} \left[ 1 + \frac{x}{|x|} \right] \rightarrow \tilde{H}(x) = \frac{1}{2} \left[ 1 + \frac{x}{|x| + \delta} \right] \quad (40)$$

where  $\delta > 0$  is a small parameter ( $10^{-3}$  or  $10^{-4}$  in practice).

**Remark 3** In the finite element implementation, the damage history variable  $r(\mathbf{x}, t)$  and the penalty regularization parameter  $\eta(\mathbf{x}, t)$  (for the elastic-damage part of the problem) on one hand, and the fields  $S$  and  $D$  (see the updates (29b,c)) (for the calcium leaching part of the problem) on the other hand, are stored in an element data base at the integration points level during the iterative process.

## 6. Numerical examples

As an illustration of the modelling framework developed in this paper, we give numerical simulations within the context of the finite element method. The algorithms developed in section 5 have been implemented in an enhanced version of the CESAR-LCPC finite element software, see (Humbert 1989). The first section concerns the simulation of a calcium leaching test under

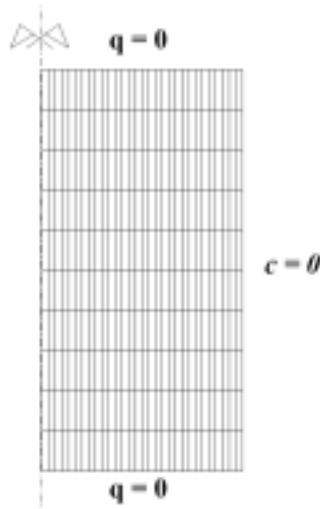


Fig. 5 The discretized cylinder and boundary conditions

ammonium nitrate, and the second section concerns mechanical tests on the chemically degraded samples of the former section. All the simulations are compared with experimental results obtained on cement paste by Carde (1996).

### 6.1. Calcium leaching under ammonium nitrate solution

We consider a cylindrical specimen of radius  $R=15$  mm and height  $h=30$  mm, and submitted to calcium leaching under ammonium nitrate solution. The discretization we use is shown in Fig. 5. Use is made of a quadratic interpolation with finite elements of equal size, i.e., equal intervals. Here, 30 intervals are used in the radial direction. This mesh will also be used for the compression simulations in section 6.2.

For the numerical simulation, an axisymmetric analysis is performed. The boundary conditions consist on zero mass fluxes on the top and bottom boundaries (the specimen is isolated there), and on imposed calcium concentration  $c=0$  [ $mol/m^3$ ] on the rest of the boundary (see Fig. 5). Of course, under these conditions, the problem becomes one-dimensional and the results are not influenced by the discretization in the axial direction.

The characteristic material data used during the computation are smoothed versions of the curves  $s(c)$ ,  $\phi(c)$  and  $\tilde{D}(c)$  shown in Figs. 1-3 to circumvent evident numerical difficulties due to the  $\delta$ -Dirac type behaviour. Note that for calcium leaching under almost demineralised water, this smoothing procedure is not necessary.

To initiate the computation, the initial condition for the calcium concentration in the liquid phase is given by  $c_0(\mathbf{x}, t=0)=2730$   $mol/m^3$  for all  $\mathbf{x} \in \Omega$  which corresponds to the initial value  $s_0(\mathbf{x}, t=0)=14700$   $mol/m^3$  for the calcium concentration in the solid phase.

Fig. 6 shows a sequence of computed calcium concentration profiles at different times of

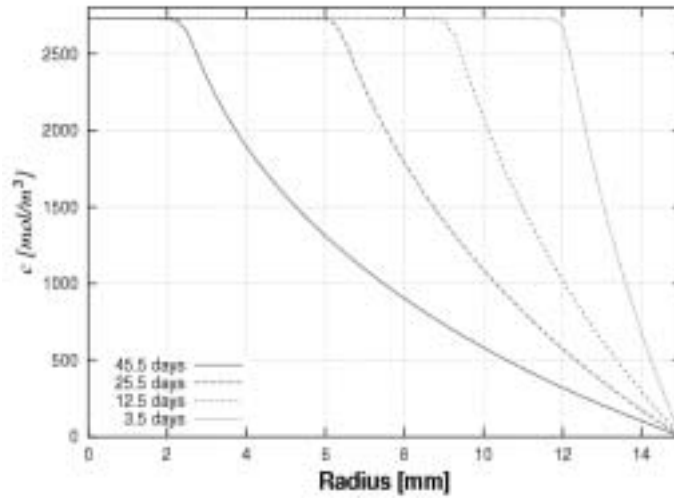


Fig. 6 Calcium concentration profile in the liquid phase at different times

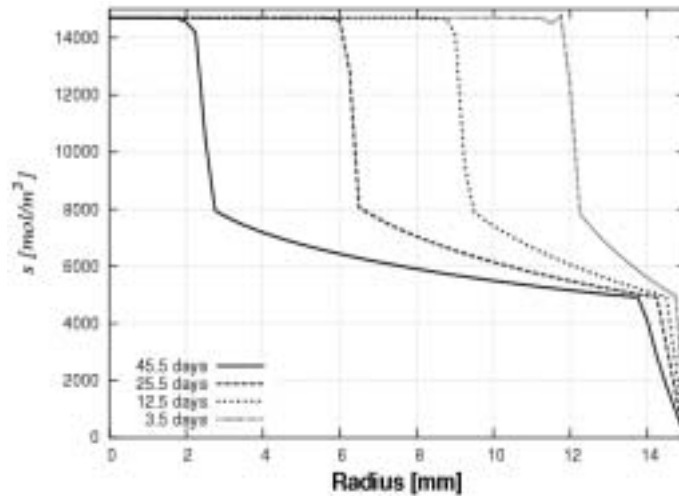


Fig. 7 Calcium concentration profile in the solid phase at different times

degradation. The corresponding profiles of calcium concentration in the solid phase  $s(c)$  are given in Fig. 7. In this latter, one can clearly identify the two dissolution fronts of the portlandite and the C-S-H phases (see Fig. 1).

In Fig. 8, we plot the evolution of the computed degraded depth versus the square root of time (in days). As expected, an almost linear relation is obtained and, moreover, it is in good adequation with the corresponding experimental results from Carde (1996).

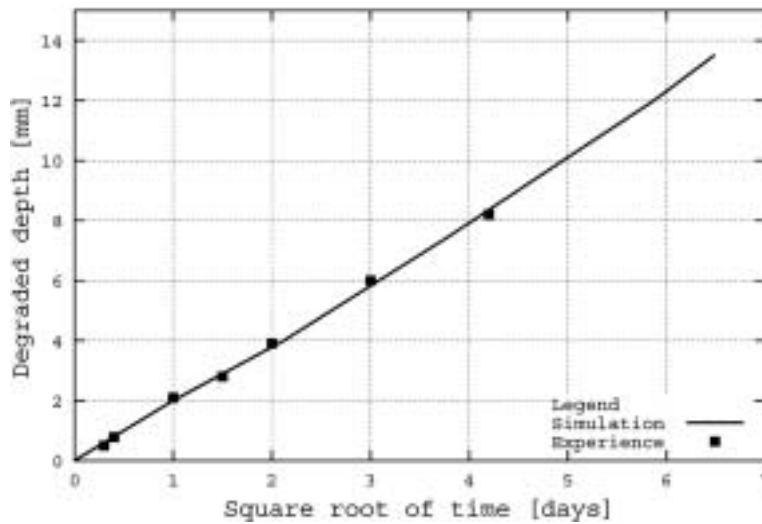


Fig. 8 Degraded depth versus the square root of time comparison with experimental data

### 6.2. Mechanical damage compression tests

The precedent cylindrical specimen is now submitted to compressive tests at different levels of calcium leaching degradation obtained from the results of the last section. Use is made of the elastic-damage model of section 3. Again, note that the chemo-mechanical coupling is present only through the Young's modulus  $E(c)$  and the first (mechanical) damage threshold  $W(c)$ .

For the elastic material data, the  $E(c)$  function is the one given in Fig. 4, with  $E(c) = E_0 = 16000$  MPa when the material is unleached and undamaged, and the Poisson's ratio is  $\nu = 0.2$ .

For the mechanical damage parameters, the first damage threshold follows the same evolution as

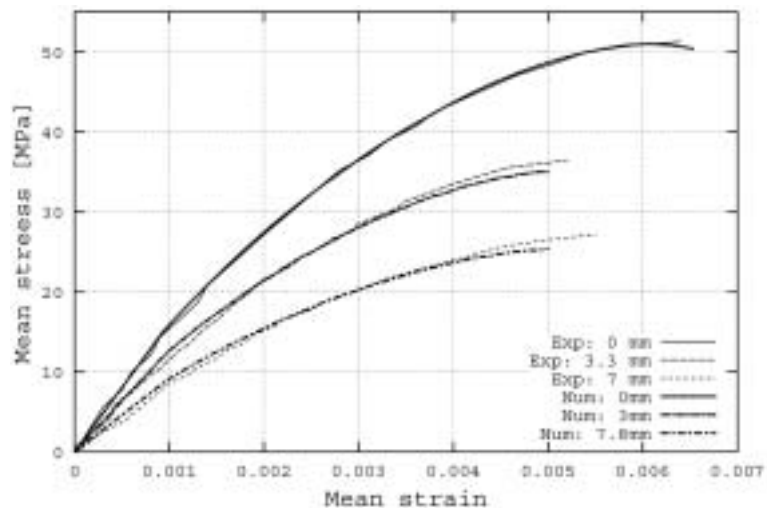


Fig. 9 Mean stress versus mean strain curves at different degraded depths

the Young's modulus:

$$W(c) = \left[ \frac{E(c)}{E_0} \right] W_0, \quad (41)$$

where, here  $W_0=5.3 \cdot 10^4$  MPa. The factor of influence of damage gradient is  $k = 0.1$  MPa.mm<sup>2</sup>.

The source of damage function  $S(\boldsymbol{\epsilon})$  (see Eqs. (14) and (17)) depends here on the positive strains and is given by:

$$S(\boldsymbol{\epsilon}) = \frac{1}{2} [\mu(c) \boldsymbol{\epsilon}^+ : \boldsymbol{\epsilon}^+ + \lambda(c) (\langle tr[\boldsymbol{\epsilon}] \rangle^+)^2] \quad (42)$$

where  $tr$  denotes the trace operator. In this work, the exponent parameter has been adapted to vary with the damage variable:  $n \equiv n(\beta)$ . That is, to make it decrease when damage grows, i.e., when  $\beta$  decreases. For the sake of simplicity, we have made the following choice:

$$n(\beta) = n_0 \beta \quad (43)$$

with  $n_0=10$  in the following computations. Of course, other functions instead of Eq. (43) can be easily adapted. One can think for example to make  $n$  depend on the source of damage function:  $n = n(S(\boldsymbol{\epsilon}))$ . Finally, the penalty parameter  $\varepsilon$  we have used in all the following computations is  $\varepsilon = 10^4$ .

The result of the compression tests for different levels of calcium leaching degradation are shown in Fig. 9. They are superposed with the experimental results of Carde (1996), see also Carde, *et al.* (1996), for different degradation depths. Again, one can see the good agreement between the numerical simulations and the experimental results. This was done already with others models, for example in Carde, *et al.* (1996), Ulm, *et al.* (1999), Torrenti, *et al.* (1998a) but by using a larger number of finite elements (10 times more for instance in Torrenti, *et al.* 1998a).

## 7. Conclusions

We have presented in this work a phenomenological modelling of the coupled chemo-mechanical degradation of cement-based materials. For the chemical part, use has been made of the well known simplified approach of calcium leaching. And for the mechanical part, continuum damage mechanics was used where the of the damage quantity is involved.

To numerically solve the calcium leaching part of the problem, we have developed an iterative solution procedure based on a relaxed linearization procedure. This choice is due to strong nonlinearity of the problem. Although its implementation was decoupled from the mechanical part of the problem, a fully coupled resolution procedure can be easily performed.

For the elastic-damage part of the problem, we have used an augmented Lagrangian formulation adapted from the recent developments given in Nedjar (2002a) within the context of the finite strains range. The advantage of this strategy is the possibility to use a simultaneous scheme to resolve this sub-problem.

Of course, other chemo-mechanical couplings than the present  $E(c)$  and  $W(c)$  couplings can be adapted. For instance, apparent calcium conductivity must also depend on mechanical damage. All the possible coupling effects are actually under investigation together with the inclusion of the plasticity in the modelling.

Finally, we have successfully simulated the experimental results of Carde (1996).

## References

- Bangert, F., Kuhl, D. and Meschke, G. (2001), "Finite element simulation of chemo-mechanical damage under cyclic loading conditions", *Fracture Mechanics of Concrete and Structures*, (R. de Borst, *et al.*, eds.), Swets and Zeitlinger, Lisse, 145-152.
- Carde, C. (1996). "Caractérisation et modélisation de l'altération des propriétés mécaniques due à la lixiviation des matériaux cimentaires", Ph. D. thesis, INSA Toulouse.
- Carde, C., François, R. and Torrenti, J. M. (1996), "Leaching of both calcium hydroxyde and C-S-H from cement paste: modeling the mechanical behaviour", *Cement Concrete Res.*, **28**(6), 1257-1268.
- Coleman, B. D. and Gurtin, M. E. (1967), "Thermodynamics with internal variables", *J. Chem. Phys.* **47**, 597-613.
- Fleck, N. A. and Hutchinson, J. W. (1993), "A phenomenological theory for strain gradient effects in plasticity", *J. Mech. Phys. Solids*, **41** (12), 1825-1857.
- Frémond, M. and Nedjar, B. (1993), "Endommagement et principe des puissances virtuelles", *C. R. Acad. Sci. Paris serie II* **317**, 857-864.
- Frémond, M. and Nedjar, B. (1996), "Damage, gradient of damage and principle of virtual power", *Int. J. Solids Struct.*, **33** (8), 1083-1103.
- Gérard, B. (1996), "Contribution des couplages mécaniques-chimie-transfert dans la tenue à long terme des ouvrages de stockage de déchets radioactifs", Ph. D. thesis, ENS Cachan.
- Humbert, P. (1989), CESAR-LCPC, un code général de calcul par éléments finis. *Bull. Liais. Labo. des Ponts et Chaussées*, **119**, 112-116.
- Le Bellégo, C., Gérard, B. and Pijaudier-Cabot, G. (2001), "Mechanical analysis of concrete structures submitted to an aggressive water", R. de Borst *et al.* (Ed.), *Fracture Mechanics of Concrete Structures*, 239-246. Swets and Zeitlinger, Lisse.
- Mainguy M., Tognazzi, C., Torrenti, J. M. and Adenot, F. (2000), "Modelling of leaching in pure cement paste and mortar", *Cement Concrete Res.*, **30**, 83-90.
- Menzel, A. and Steinmann, P. (2000), "On the continuum formulation of gradient plasticity for single and polycrystals", *J. Mech. Phys. Solids*, **48**, 1777-1796.
- Mühlhaus, H. B. and Aifantis, E. C. (1991), "A variational principle for gradient plasticity", *Int. J. Solids Struct.* **28**, 845-857.
- Nedjar, B. (2001), "Elastoplastic-damage modelling including the gradient of damage: formulation and computational aspects", *Int. J. Solids Struct.*, **38**, 5421-5451.
- Nedjar, B. (2002a), "A theoretical and computational setting for a geometrically nonlinear gradient damage modelling framework", *Comput. Mech.*, **30**, 65-80.
- Nedjar, B. (2002b), "An enthalpy-based finite element method for nonlinear heat problems involving phase change", *Comput. Struct.*, **80**, 921.
- Polizzoto, C. and Borino, G. (1998), "A thermodynamics-based formulation of gradient dependent plasticity", *Eur. J. Mech., A/Solids*, **17**, 741-761.
- Simo, J. C. and Laursen, T. A. (1992), "An augmented lagrangian treatment of contact problems involving friction", *Comput. Struct.*, **42**(1), 97-116.
- Tognazzi, C. (1998), "Couplage fissuration dégradation chimique dans des matériaux cimentaire: caractérisation et modélisation", Ph. D. thesis, INSA Toulouse.
- Torrenti, J. M., Adenot, F., Tognazzi, C., Danese, S. and Poyet, S. (1998a), "Application du modèle de dégradation du béton au cas des milieux fissurés et au couplage avec la mécanique", *Concrete: from Material to Structure Proceedings of the International RILEM Conf.* Arles.
- Torrenti, J. M., Didry, O., Ollivier, J. P. and Plas, F. (1999), *La dégradation des bétons couplage fissuration-dégradation chimique*, Hermès.
- Torrenti, J. M., Mainguy, M., Adenot, F. and Tognazzi, C. (1998b), "Modelling of leaching in concrete", In R. de Borst, N. Bicanic, H. Mang, and G. Meschke (Eds.), *Proc. Euro-C 98, Computational Modelling of Concrete Struct.*, 531-538. Balkema, Rotterdam, The Netherland.

Ulm, F. J., Lemarchand, E. and Heukamp, F. H. (2002), "Elements of chemomechanics of leaching of cement-based materials at different scales", *Eng. Frac. Mechanics in press*.

Ulm, F. J., Torrenti, J. M. and Adenot, F. (1999), "Chemoporoplasticity of calcium leaching in concrete", *Eng. Mech., ASCE*, **125**(10), 1200-1211.

CC